

Palaeobiological and geochemical aspects of reptilian coprolites from a Maastrichtian Deccan volcano-sedimentary intertrappean deposit of central India

Vivesh V Kapur^{1,2}, Ramanand Sagar^{1,2}, Kamlesh Kumar^{1,2}, Amritpal Singh Chaddha¹,
Ranjit Singh Lourembam³, Anshika Mishra¹, and Anupam Sharma¹

¹Birbal Sahni Institute of Palaeosciences

²Academy of Scientific and Innovative Research (AcSIR)

³Centre for Advanced Studies in Geology, Panjab University

April 16, 2023

This paper is a working manuscript, under preparation for submission to a peer reviewed journal.

1 **Palaeobiological and geochemical aspects of reptilian coprolites from a Maastrichtian**
2 **Deccan volcano-sedimentary intertrappean deposit of central India**
3

4 Vivesh V. Kapur^{a,b*}, Ramanand Sagar^{a,b}, Kamlesh Kumar^{a,b}, Amritpal Singh Chaddha^a,
5 Ranjit Singh Lourembam^c, Anshika Mishra^{a, d}, Anupam Sharma^a

6 ^a Birbal Sahni Institute of Palaeosciences, 53, University Road, Lucknow 226007, India.

7
8 ^b Academy of Scientific and Innovative Research (AcSIR), Ghaziabad 201002, India.

9
10 ^c Centre for Advanced Studies in Geology, Panjab University, Chandigarh 160014, India.

11
12 ^d B-471, Rajajipuram, Lucknow 226017, India.

13
14

15

16

17

18

19

20

21

22

23

24

25

26 * Corresponding author: Vivesh V. Kapur (Orcid ID: 0000-0001-6542-5964)

27 Email: viveshkapur@gmail.com; viveshvir_kapur@bsip.res.in

28 **ABSTRACT**

29 Cretaceous-Paleogene coprolite (fossilized faecal matter) records are significant in terms of
30 providing direct palaeobiological evidence (as inclusions) in order to understand the diet and
31 linkage(s) to producer animal(s). In the past >150 years, research investigations (in India)
32 have focussed on the Maastrichtian Type-A coprolite morphotype (linked to titanosaurid
33 dinosaurs). Consequently, scanty information is available on the overall assemblage of Indian
34 Maastrichtian vertebrate coprolites in terms of their morphological diversity, chemical
35 composition, biotic-abiotic inclusions in the context of producer linkage(s) and geographic
36 distribution within the Deccan volcano-sedimentary infra- and intertrappean deposits of
37 India. Therefore, we here present a detailed record of a coprolite assemblage from the
38 Maastrichtian intertrappean deposits of Lotkheri, central India. The investigated coprolite
39 assemblage consists of five morphotypes based on their geometry, surface, and internal
40 textures. Biotic inclusions suggest that chelonians and crocodiles are the most likely producers
41 of these ichnofossils. The associated faunal remains of chelonians and crocodylians support
42 the proposed producer linkages. Bite marks of Gar fish (genus *Lepisosteus*) observed on the
43 external surface of a few coprolite specimens (studied herein) are rare in the global fossil
44 records. The analytical evidences confirm the phosphatic composition of the coprolites with
45 the unique presence of three distinct morphologies (i.e., spherical, rods, and needles) of
46 hydroxyapatite crystal inclusions that are explained with the help of a chemical ‘Growth Unit
47 Model’.

48 **Keywords:** Chelonians, Crocodiles, Hydroxyapatite, Ichnofossils, Palaeodiet

49

50

51

52 **INTRODUCTION**

53 Coprolites (fossilised faecal matter) have been significantly utilized in several research
54 studies to reconstruct past ecosystems and to understand the dietary habit(s) of prehistoric
55 fauna (Richter & Baszio 2001a, 2001b; Chin 2002; Prasad et al. 2005; Zatoń et al. 2015;
56 Khosla et al. 2015; Vajda et al. 2016; Chin et al. 2017; Qvarnström et al. 2017; Dentzien-Dias
57 et al. 2018; Barrios-de Pedro et al. 2018; Bajdek & Bienkowska-Wasiluk 2020; Rummy et al.
58 2021; Yao et al. 2022). In this regard, vertebrate coprolites from the Cretaceous-Paleogene
59 (K-Pg) interval are known to be significant in order to understand the change(s) in
60 palaeodietary preference(s) of producer taxa and their surrounding palaeoecological
61 condition(s) (Suazo et al. 2012) considering the prevalence of stressed climatic and/or
62 environmental conditions near the K-Pg time-slice. It is generally argued that the climatic
63 change(s) close to the K-Pg interval occurred as a result of a meteorite impact (at Chicxulub,
64 Mexico) and/or extensive volcanic activity (e.g., Deccan Trap volcanism in India) (see Keller
65 et al. 2020 and references therein). The Deccan volcanic activity occurred in three
66 episodes/phases and straddled the K-Pg boundary spanning at least >5 million years (from 69
67 Ma to 63 Ma) (Pande 2002; Self et al. 2008; Schoene et al. 2015; Fantasia et al. 2016; Keller
68 et al. 2020). The Maastrichtian Deccan Volcano Sedimentary Sequences (DVSS) i.e., the
69 infratrappean (Lameta Formation) and the intertrappean deposits have yielded abundant data
70 on various fossil vertebrate groups that include fish, reptiles, amphibians, and mammals
71 (Kapur and Khosla 2019 and references therein). However, we have limited knowledge on
72 Maastrichtian vertebrate coprolites in terms of their morphological diversity, chemical
73 composition, biotic-abiotic inclusion(s), producer linkage(s), and geographic distribution
74 within the DVSS in India. This is owing to but not limited to the following factors: a)
75 sporadic and limited occurrence of DVSS, b) plausible preservation bias between coprolite
76 ichnofossils and vertebrate body fossils, and c) scarce palaeontological efforts for the

77 recovery of coprolite ichnofossils within DVSS. Thus, much emphasized are the
78 Maastrichtian Type-A coprolite morphotype (linked to titanosaurid dinosaurs) limited to an
79 infratrappean (Lameta Formation) horizon at Pisdura locale, central India (Matley 1939;
80 Prasad et al. 2005; Khosla et al. 2015; also refer to Table 1 in Kapur et al. 2020).
81 Additionally, Maastrichtian ‘intertrappean’ coprolite data, to date, is represented by a single
82 morphotype and limited to the Lotkheri locale, central India (refer to Kapur et al. 2006).
83 Further, previously recorded reptilian coprolites (in particular, the ones linked to chelonians
84 and crocodiles) from the infratrappean Pisdura locale (Matley, 1939) and the intertrappean
85 deposits of Lotkheri (Kapur et al., 2006) have not been analysed, for their biotic/abiotic
86 inclusions, and geochemical composition. The above-mentioned aspects do hamper our
87 understanding on the morphometric/morphotaxonomic diversity of coprolite records from the
88 Maastrichtian of India, the dietary habit(s) of the producer animal(s), and in a few cases
89 envisaged association(s) of previously reported coprolites to producer taxa. We herein present
90 a detailed account on coprolite assemblage recovered from a Maastrichtian intertrappean
91 deposit at Lotkheri, central India. Data on biotic inclusion(s) assisted to infer the likely
92 producer(s) and the producer(s) dietary habit(s). Analytical techniques helped to decipher the
93 chemical composition of the recovered coprolites, host (coprolite-yielding), and associated
94 lithologies. Finally, an attempt has been made to explain the unique presence of a variety of
95 morphologies of hydroxyapatite crystal (observed as coprolite inclusions) in the context of a
96 chemical model.

97 **GEOLOGICAL SETTING AND AGE**

98 All the coprolites recorded in the present study were recovered as surface collections from an
99 intertrappean site (geographic co-ordinates: N 24°29'; E 75°43') located ~0.5 km south of the
100 village Lotkheri (also known as ‘Lotkhedi’), Bhanpura Tehsil, Mandsaur District, Madhya
101 Pradesh State, central India (Figs. 1a-e). The sedimentary succession exposed at the Lotkheri

102 locality comprises a 0.75 m to 1.5 m variably thick unfossiliferous red clays overlain by a
103 0.30 m to 0.65 m ossiferous (coprolite- and vertebrate-yielding) grey-green clays (Figs. 1b-d).
104 Underlying weathered basalts can be observed both in a nala section as well in a dug well
105 within the vicinity of the Lotkheri fossil locale that hint at the ‘intertrappean’ nature of the
106 studied sedimentary succession (Figs. 1e). Published literature suggest an absence of
107 infratrappean (Lameta Formation) sediments in the vicinity of the investigated locality while
108 the Deccan Traps are underlain by Vindhyan or the Lower Gondwana (Antroli Formation,
109 equivalent to Talchir Boulder Beds) sediments (Kapur et al. 2006 and references therein).
110 Based on the widely occurring intertrappean faunal remains (i.e., the presence of fish dental
111 remains assigned to *Igdabatis indicus*, fish scales belonging to *Lepisosteus indicus*,
112 chelonians and crocodilian remains) the Deccan volcano-sedimentary intertrappean deposits
113 at Lotkheri are considered to be Maastrichtian in age (Kapur et al. 2006).

114 **MATERIAL AND METHODS**

115 Surface prospecting at Lotkheri intertrappean site yielded a total of fourteen coprolite
116 specimens, a rarity in terms of the coprolite data from the Maastrichtian ‘intertrappean’
117 horizons of India. The collected coprolite specimens were individually photographed with the
118 help of a digital camera (Model: Nikon D5200) and measured using a Dial Vernier Calliper.
119 The specimens were individually examined for external structures under a binocular
120 microscope (Model: Leica S8APO) in the Vertebrate Palaeontology and Preparation
121 Laboratory (VPPL), Birbal Sahni Institute of Palaeosciences (BSIP), Lucknow, India. Before
122 the thin section, Scanning Electron Microscopy (SEM) and chemical analyses, the individual
123 coprolite specimens were disinfected in a Sodium Perborate Monohydrate solution. To
124 examine coprolite inclusions under an automated slide scanner (Model: Grundium Ocus
125 MGU-00001) at VPPL, thin sections (30 µm thick and transverse to the long axis) of the
126 coprolite specimens were prepared. Separately, a few coprolite specimens were chemically

127 examined utilizing Energy Dispersive Spectroscopy (EDS) (at multiple spots) and a Scanning
128 Electron Microscope (Model: JEOL7610F) under the acceleration voltage of 15kv and
129 variable (6-9 A) current with EDAX (Model: Octane Plus with TEAM software version
130 V4.2.1) at BSIP, Lucknow, India. Prior to XRD analysis, the coprolite specimens were
131 cleaned utilizing an ultrasonic cleaner. Individual coprolite specimens, associated- (LTK-1)
132 and host-lithology (LTK-2) samples were grounded up to 74 μ m. All the grounded
133 specimens/samples were analysed using Panalytical X'pert³ powder diffractometer
134 equipment, working at 45 KV & 40 mA. The XRD measurements were carried out from 5° to
135 70° (2 θ) range with a step size of 0.010° and time per step 30s with a scan speed of 0.090°/s
136 using Cu as X-ray source ($K\alpha=1.5405\text{\AA}$) at the BSIP, Lucknow, India. The mineral
137 identification was carried out by the X'pert high score (<https://www.malvernpanalytical.com>)
138 and ICDD PDF-4 mineral database (Gates-Rector and Blanton 2019). In addition, the two
139 sediment samples (i.e., LTK-1 & LTK-2) were analysed by the X-ray Fluorescence (XRF)
140 technique (WD-XRF Model: axios max, 4 KW, PANalytical) at BSIP, Lucknow, India. The
141 precision and accuracy of the sample preparation and instrumental performance were checked
142 using international reference standards of sediments (e.g., BCR-2, SGR-1b, RGM-2 and
143 DGH). The accuracy of measurement is better than 2–5% and precision <2. EDS reports of
144 the investigated coprolites are provided as Supplementary Data S1. The specimens and slides
145 relating to the coprolite specimens investigated herein are housed at BSIP, Lucknow, India
146 (BSIP locality no. 10145; Specimens nos. BSIP 42253-42282; Museum slide nos. 17250-
147 17251).

148 **RESULTS**

149 *Morphological Characterization*

150 A total of fourteen coprolite specimens [specimen nos. LTK/2101-154 (BSIP 42254),
151 LTK/2101-234 (BSIP 42255), VVK/BNP/GEO2 (BSIP 42256), VVK/BNP/GEO1 (BSIP
152 42253), LTK/2101-194 (BSIP 42258), LTK/2101-351 (BSIP 42260), VVK/BNP/GEO12
153 (BSIP 42257), LTK/2101-321 (BSIP 42261), LTK/2101-14 (BSIP 42259), LTK/2101-88
154 (BSIP 42262), LTK/2101-21 (BSIP 42263), LTK/2101-15 (BSIP 42265), VVK/BNP/GEO9
155 (BSIP 42264), VVK/BNP/GEO10 (BSIP 42266)] representing five morphotypes (M1-M5) are
156 described in the present investigation (Figs. 2-3). It should be noted that the investigated
157 coprolites specimens were recovered in association with vertebrates including fishes (mainly
158 scales including those belonging to the genus *Lepisosteus indicus*), chelonians (carapace
159 fragments and vertebrae), and crocodylians (scutes and isolated teeth) (Fig. 4).

160 *Morphotype M1*: Four coprolite specimens [specimen nos. VVK/BNP/GEO1 (BSIP 42253),
161 LTK/2101-154 (BSIP 42254), LTK/2101-234 (BSIP 42255), VVK/BNP/GEO2 (BSIP
162 42256)] represent morphotype *M1* (Figs 2a-d). The morphotype *M1* depicts whitish to pale
163 yellow colouration, with an average length of 26.46 mm and an average width of 23.17
164 mm (refer to Table 1), spherical with rounded to sub-rounded outline (length/width ranging
165 from 0.92 mm to 1.25 mm; Table 1), are circular/sub-circular in cross-section, with external
166 surface generally smooth that may possess a few pits and/or desiccation cracks, depict biotic
167 inclusions consisting of both plant remains and partially digested bone content (refer to
168 section '*Abiotic and biotic inclusions*') and are chemically phosphatic (refer to section '*XRD
169 and XRF analyses*').

170 *Remarks*: This is the first record of large (cm-sized) spherical (with rounded to sub-rounded
171 outline) coprolites from India i.e., morphotype *M1* is morphologically different from the
172 previously known Mesozoic-Cenozoic coprolites from India (refer to Kapur et al. 2020).
173 Global records suggest that spherical-shaped coprolites (with rounded to sub-rounded
174 outlines) have been earlier recorded from the Lower Triassic limestone unit (part of the

175 Lower Gogolin Beds representing a shallow-water coastal palaeodepositional environment)
176 in a quarry section, Upper Silesia, southern Poland (refer to Fig. 4B in Brachaniec et al.
177 2015). The coprolites recorded by Brachaniec et al. (2015) have been linked to
178 sauropterygian reptiles based on the presence of vertebrate remains (as inclusions) and
179 associated faunal remains. Further, the spherical coprolites (see Brachaniec et al. 2015) are at
180 least 2 times smaller (being ~1 cm in diameter) compared to the morphotype M1 recorded
181 herein. Upper Triassic (Rhaetian) lacustrine mudstone unit belonging to the Kap Stewart
182 Formation, East Greenland is also known to yield somewhat spherical-shaped coprolites (see
183 Figs. 4d-g in Hansen et al. 2015) that preserve bone material (thus linked to unidentified
184 carnivore) and approximately 50% smaller than morphotype M1 recorded from Lotkheri
185 locale. Lucas et al. (2012) previously recorded ‘rounded’ (however, in polar view) coprolites
186 (tentatively assigned to *Alococopros triassicus*) from the late Eocene marginally lacustrine
187 sandy shale unit along the Aksyir River, Zaysan Basin, Kazakhstan. However, *Alococopros*
188 *triassicus* recorded from Zaysan Basin differs from morphotype M1 in being smaller (length
189 ~16-23 mm; maximum diameter 9-16 mm) and having longitudinal striations. Recently,
190 Muftah et al. (2020) recorded spherical coprolites from the Neogene (late Miocene) Sahabi
191 Formation (Sirt Basin, Libya) that are smaller in size (i.e., diameter ranging from 14 mm to
192 19.5 mm) in comparison to morphotype M1 recorded in our study. Spherical scats are known to
193 be produced by extant gharials (*Gavialis gangeticus*) that are quite similar in size (~20 mm in
194 diameter) to the coprolite morphotype M1 recorded in the present investigation (see
195 Milàn 2012). However, the presence of biotic inclusions in the form of both plant and
196 undigested bone matter within morphotype M1 coprolites (refer to section ‘Biotic and abiotic
197 inclusions’, this study) suggests that morphotype M1 were most likely produced by
198 omnivorous chelonians as opposed to exclusively carnivorous crocodiles (for details refer to
199 section ‘Discussion’).

200 *Morphotype M2*: This morphotype is represented by the five specimens: VVK/BNP/GEO12
201 (BSIP 42257), LTK/2101-194 (BSIP 42258), LTK/2101-351 (BSIP 42260), LTK/2101-321
202 (BSIP 42261)(Figs 2e-i)that are whitish to pale yellow coloured, with an average length of
203 25.53 mm and an average width of 26.03 mm(refer to Table 1), tear-drop shaped (with
204 length/width ranging from 0.61 mm to 1.46 mm; Table 1), anisopolar with one end slightly
205 tapered/arched due to a conspicuous inclination along its longitudinal axis on one side,
206 elliptical in cross-section, external surface generally smooth that may possess pits and/or
207 desiccation cracks, showcase biotic inclusions consisting of both plant remains, partially
208 digested bone content (refer to section '*Biotic and abiotic inclusions*') and phosphatic in
209 chemical nature (refer to section '*XRD & XRF analyses*').

210 *Remarks*: This is one of the most common morphotype observed at the Lotkheri locale (Figs
211 2e-i) and was previously illustrated by Kapur et al. (2006). Kapur et al. (2006) linked the
212 recovered coprolites (single morphotype) to Archosauria due to the associated presence of
213 vertebrate remains of both crocodiles and turtles [refer to Plate 1 (Fig. 26) in Kapur et al.
214 2006]. However, the author did not attempt to analyse the Lotkheri coprolites for biotic-
215 abiotic inclusions and/or geochemically. Apart from the Lotkheri locale, published records
216 from India suggest that the teardrop-shaped anisopolar (one end slightly tapered/arched due
217 to a conspicuous inclination along its longitudinal axis on one side) coprolites have not been
218 recorded previously from the Mesozoic [particularly from the Maastrichtian infratrappean
219 (Lameta Formation) deposits at Pisdura locale, central India (see Matley 1939)]. We observe
220 a slight morphological resemblance of morphotype M2 with coprolites assigned to 'Group
221 2(Type A) Morphotype' by Sharma and Patnaik (2010) from the Miocene Baripada beds of
222 Orissa, India (refer to Fig. 2b in Sharma and Patnaik 2010). These authors also recorded a
223 'Tear-Drop shaped' coprolite (linked to crocodiles) that measures 2.1 cm in diameter (refer to
224 Fig. 2a in Sharma and Patnaik 2010); however, the illustrated specimen is broken to allow

225 comparison with morphotype M2 coprolites reported in our study. Inclusions of both plant
226 and bone matter within morphotype M2 coprolites (refer to section '*Biotic and abiotic*
227 *inclusions*') hint at an omnivorous producer that is most likely chelonians (as detailed in
228 section '*Discussion*'). Interestingly, a few specimens assigned to morphotype M2 showcase
229 bite marks on the external surface (Figs. 2g, 2i1) that we herein link to the garfish genus
230 *Lepisosteus* (for details refer to section '*Discussion*'). Global records exist on Upper
231 Cretaceous vertebrate coprolites (Waldman 1970; Broughton et al.1978; Nobre et al. 2008;
232 Hollocher et al. 2010; Suoto 2010; Hunt et al. 2012, 2015; Sullivan & Jasinski 2012; Suozo et
233 al. 2012; Godfrey & Palmer 2015; Milán et al. 2015; Schwimmer et al. 2015; Brachaniec &
234 Wiczorek 2016; Segesdi et al. 2017); however, none of these are morphologically
235 comparable to morphotype M2 recorded in the present investigation.

236 *Morphotype M3*: Morphotype M3 is represented by the following specimens: LTK/2101-88
237 (BSIP 42262), and LTK/2101-21 (BSIP 42263) (Figs. 3a1-a2, b1-b3). Morphotype M3
238 coprolites are generally whitish to pale yellow coloured, elliptical with an average length
239 measuring 29.71 mm and average width measuring 22.58 mm (Table 1), anisopolar, display
240 constrictions, with burrows/pits and/or desiccation cracks generally observed on the external
241 surface, and geochemically calcium phosphatic.

242 *Remarks*: Coprolites morphologically similar to Morphotype 3 (recorded herein) have not
243 been reported previously from the Mesozoic (e.g., Jurassic Kota Formation, Triassic Maleri
244 Formation, Maastrichtian infra- and intertrappean sediments) and the Cenozoic (Lutetian
245 Harudi Formation, Aquitanian Khari Nadi Formation, Burdigalian-Langhian Chassra
246 Formation, and the Burdigalian Baripada beds) time intervals of India. The presence of biotic
247 inclusions in the form of both plant and undigested bone matter within morphotype M3
248 coprolites (refer to section '*Biotic and abiotic inclusions*') suggests that morphotype M3 were
249 most likely produced by omnivorous chelonians as opposed to exclusively carnivorous

250 crocodiles (for details refer to section '*Discussion*'). Reptilian coprolites within the size range
251 of Morphotype 3 (this study) are well-known to occur within the Upper Cretaceous
252 sedimentary succession across the globe (Waldman 1970; Broughton et al. 1978; Nobre et al.
253 2008; Hollocher et al. 2010; Suoto 2010; Hunt et al. 2012, 2015; Sullivan & Jasinski 2012;
254 Suozo et al. 2012; Godfrey & Palmer 2015; Milán et al. 2015; Schwimmer et al. 2015;
255 Brachaniec & Wieczorek 2016; Segesdi et al. 2017); however, they do not compare in
256 general shape depicted by Morphotype 3.

257 *Morphotype 4:* We herein assign specimen nos. LTK/2101-15 (BSIP 42265), and
258 VVK/BNP/GEO9 (BSIP 42264) to Morphotype 4 (Figs.3c1-c2, d). Morphotype 4 coprolites
259 display pale yellow to reddish brown colouration, cylindrical but curved along the
260 longitudinal axis, average length measuring 40.42 mm, average width measuring 30.93 mm
261 (Table 1), having burrows/pits and/or desiccation cracks on the external surface, and calcium
262 phosphatic in chemical nature.

263 *Remarks:* Thin sections of the Morphotype 4 coprolites (refer to section '*Biotic and abiotic*
264 *inclusions*') suggests that these ichnofossils were most likely produced by crocodiles rather
265 than chelonians (for details refer to section '*Discussion*'). Coprolite records from India
266 suggest that the ichnofossils linked to crocodiles have been recorded previously from the
267 Lutetian Harudi Formation, Kachchh region, western India [refer to Plate II (Figs.7-8) in
268 Sahni and Mishra 1975]; however, incomplete nature of specimen nos. LTK/2101-15 (BSIP
269 42265) and VVK/BNP/GEO9 (BSIP 42264) do not allow direct comparisons with Harudi
270 coprolites, at this stage. A common occurrence of coprolites linked to crocodiles within the
271 Upper Cretaceous sedimentary successions of the globe has been observed in the published
272 literature (Hunt et al. 2012, 2015 and references therein); however, due to fragmentary nature
273 of specimens assigned to Morphotype 4, direct comparisons are not possible at this stage.

274 *Morphotype 5*: This morphotype is represented by a single complete specimen
275 VVK/BNP/GEO10 (BSIP 42266) (Figs. 3e1-e2). Morphotype 5 displays a pale yellowish
276 white colouration, irregularly folded, measuring 36.66 mm in length and 13.33 mm in width
277 (Table 1), anisopolar with both ends pinched and tapered, displaying constrictions forming
278 conspicuous lobes and having desiccation cracks on the external surface(Figs. 3e1-e2).

279 *Remarks*: The specimen VVK/BNP/GEO10 (BSIP 42266) has not been analysed for biotic-
280 abiotic inclusions through thin section techniques and/or analysed chemically. A separate
281 detailed investigation utilizing the non-destructive micro-CT analysis is underway to link the
282 specimen VVK/BNP/GEO10 (BSIP 42266) to its producer. However, the presence of
283 constrictions that form conspicuous lobes strongly points towards an organic origin (refer to
284 Hantzschel et al. 1968; Broughton et al. 1978). Further, the common presence of crocodilian
285 and chelonian remains at Lotkheri (Fig. 4) suggests that Morphotype 5 was most likely
286 produced by a reptilian. Interestingly, none of the previously recorded coprolite morphotypes
287 or ichnotaxa recorded within the Mesozoic-Cenozoic sediments of India is comparable to
288 Morphotype 5. In terms of global records on coprolites, irregularly folded coprolites recorded
289 from the late Cretaceous Whitemud Formation, Canada [refer to Plate 43 (Fig. 18) Broughton
290 et al., 1978] are morphology quite comparable to the Morphotype 5 (this study); however, the
291 Canadian coprolites either display longitudinal striations or polygonal cracks on their external
292 surfaces unlike Morphotype 5 from Lotkheri, central India. Amstutz (1958) recorded four
293 coprolite specimens from the ‘Tertiary’ sediments of Salmon Creek, Washington, USA. Of
294 these, one of the unnamed morphotype specimens is almost identical to Morphotype 5,
295 recorded herein. However, the coprolite record by Amstutz (1958) may be doubted due to
296 chemical analysis showing iron being the major chemical component of the specimen with a
297 complete absence of phosphorous (refer to pp.11-12 in Hantzschel et al. 1968). An irregular
298 morphotype “Ichnotaxon I” represented by a single specimen (that displays the presence of

299 three lobes on the outer surface with desiccation cracks) from the Late Miocene of Egypt
300 [refer to Plate II (Fig.5) in Muftah et al. 2020] is quite comparable to Morphotype 5 from
301 Lotkheri. However, “Ichnotaxon I” of Muftah et al. (2020) is at least two times larger than
302 specimen no. VVK/BNP/GEO10 (BSIP 42266).

303 *Biotic and abiotic inclusions*

304 It should be noted that the present investigation reveals for the first time the internal texture,
305 abiotic and biotic inclusions within a collection of vertebrate coprolites from a Maastrichtian
306 intertrappean deposit in India (i.e., Lotkheri) utilizing both scanning electron microscopy
307 (Figs. 5-6) and digital scanning of thin sections (Fig. 7). We observe the presence of micron-
308 sized porous structures (or ‘vesicles’), and walled egg-like mineral spheres (or
309 ‘microspherulites’) (Figs. 6e-f) within the investigated coprolites. The observed porous
310 structures are generally considered as a reminiscence of escaping gases during the process of
311 decomposition of the faecal matter (Lamboy et al. 1994; PurnachandraRao & Lamboy 1995;
312 Northwood 2005; Kapur et al. 2020; Sagar et al. 2022). The microspherulites (i.e., egg-like
313 mineral spheres) are commonly ascribed to mineral pseudomorphs of sulphur-producing
314 bacteria (Hollocher et al. 2010; Owocki et al. 2013; Bajdek et al. 2016; Kapur et al. 2020;
315 Sagar et al. 2022). Additional biotic remains observed within the Lotkheri coprolites include
316 remains of freshwater sponge spicule morphotype *Acanthoxea* (Fig. 7c, 7g), possible dung
317 beetle eggs (Figs. 7d-e) and some burrow structures (Fig. 7i) (also refer to section
318 ‘*Discussion*’).

319 SEM analyses show the dominant presence of phosphatic (Hydroxyapatite - HAP) crystals
320 (Figs. 6, 8) in the coprolite morphotypes recorded herein. The multi-spot EDS examination of
321 the HAP crystals indicates a high concentration of Ca, P, and O. Interestingly, the HAP
322 crystals showcase three distinct morphologies: spherical (HAP-S), rod-like (HAP-R), and
323 needle-like (HAP-N) (Figs. 6, 8) (also refer to section ‘*Discussion*’).

324 *XRD and XRF analyses*

325 Bulk mineralogical data based on the XRD results show that the eight analysed coprolite
326 specimens are dominantly comprised of Hydroxyapatite apart from the presence of other
327 accessory minerals such as Barite, Quartz and Feldspar (Fig. 9a-b). However, XRD data on
328 the lithological samples suggest the minerals Feldspar, Quartz, and Plagioclase occur in a
329 decreasing order of preponderance in terms of percentage (Fig. 9c). Additionally, the
330 minerals Feldspar, Quartz, and Plagioclase within the coprolite-yielding host-lithology
331 sample LTK-2 are present in lesser proportion compared to that in the unfossiliferous sample
332 LTK-1 (Fig. 9c). Considering the XRF data on major oxides the relative composition (in %)
333 concerning SiO₂, Al₂O₃, Fe₂O₃, Na₂O, and K₂O within sample LTK-1 is less as compared to
334 that in coprolite-yielding sample LTK-2 (Fig. 9d). This observation is also substantiated by
335 the mineral composition shown in the XRD spectra. Further, the enrichment of SiO₂ and
336 Fe₂O₃ in the sample LTK-1 indicates more sediment-water interaction that may have been
337 unfavourable for coprolite preservation within LTK-1 sediments. In contrast, the sample
338 LTK-2 showcasing a relatively high percentage of SiO₂, Al₂O₃, Na₂O, and K₂O favours the
339 preservation of fossils including the coprolites recorded herein. Geochemical data corroborate
340 field and laboratory palaeontological efforts carried out on the unfossiliferous red clay sample
341 LTK-1 and fossiliferous (coprolite and vertebrate yielding) grey clay sample LTK-2.

342 **DISCUSSION**

343 Reptilian coprolites from the Maastrichtian intertrappean deposit of Lotkheri (central India)
344 reveal the presence of five morphotypes (i.e., spherical-M1, tear-drop shaped-M2, elliptical-
345 M3, cylindrical-M4 and irregularly folded-M5) based on their geometry, surface, and internal
346 textures. The common presence of undigested bone matter (Figs. 5a1, 5b1, 5c1, 5d,
347 5e1) including the presence of fish scales (Figs. 7a-b) apart from plant remains (Fig. 7f, 7h)
348 within a few investigated coprolites (mainly within morphotypes M1, M2, M3) supports an

349 omnivorous diet of the producer. Several extant chelonians species belonging to the family
350 Trionychidae (i.e., *Amydacartilaginea*, *Nilssonia gangeticus* (= *Aspideretes gangeticus*),
351 *Nilssoniahurum* (= *Aspidereteshurum*), *Trionyxtriunguis*) that generally dwell in freshwater
352 ponds and/or rivers have been documented to consume an omnivorous diet (Jensen & Das
353 2008 and references therein). Recovery of chelonian remains (Figs. 4a-b) in association with
354 the coprolites (recorded herein) further supports our inference that the producers of
355 morphotypes M1-M3 were chelonians (also refer to section “*Morphological*
356 *characterization*”). The absence of bone matter within morphotype M4 coprolite specimen
357 LTK/2101-15 (BSIP 42265) suggests that the producer animal had an effective digestive
358 system compared to chelonians. Extant crocodiles are known to have an effective digestive
359 system (i.e., having stomach acid with a pH value up to ~2 and in a volume quite higher
360 compared to other carnivores in the animal kingdom) to allow complete digestion of
361 vertebrate remains (Fisher 1981; Coulson et al. 1989; Trutnau & Sommerlad 2006;
362 Balaguera-Reina et al. 2018 and references therein). In a separate study on modern
363 crocodilians, Milàn (2012) observed a complete absence of skeletal remains in the scats of
364 crocodiles that were provided with a diet comprising of piglets, fish and chicken. Numerous
365 crocodilian elements in the form of scutes and isolated teeth (Figs. 4c-l) were recovered from
366 Lotkheri intertrappean deposits in association with coprolites during the present investigation
367 (also refer to Kapur et al. 2006). Thus, it is quite likely that crocodiles are the producers of
368 the morphotype M4 coprolites. Due to the reasons mentioned earlier, Morphotype 5 specimen
369 no. VVK/BNP/GEO10 (BSIP 42266) was excluded from the destructive analyses; however,
370 its morphology and associated faunal remains hint at a reptilian producer. Additional, biotic
371 inclusions observed within the Lotkheri coprolites include remains of freshwater sponge
372 spicule morphotype *Acanthoxea*, possible dung beetle eggs and some backfilled burrow
373 structures. Fresh water sponge spicules (in particular, morphotype *Acanthoxea*) have been

374 previously recorded within the Maastrichtian Type-A coprolites (linked to titanosaurid
375 sauropods) from the infratrappean (Lameta Formation) deposits of Pisdura, central India
376 (Khosla et al. 2015) and recently within the Miocene chelonian coprolites from Kachchh
377 region, western India (Sagar et al. 2022). Many extant dung beetle species (e.g., *Onthophagus*
378 *gazella*) are known to form tunnels/burrows structures to sustain brood chambers (Chin and
379 Gill 1996 and references therein). It is observed that the pattern and size of the burrows and
380 brood chambers are unique to extant species of dung beetles; however, it is difficult to link
381 these inclusive structures to a particular taxon in the case of deep-time fossilized faecal
382 matter i.e., coprolites (Chin & Gill 1996 and references therein). The presence of burrow
383 structures, dung beetle eggs, and soft parts of beetles within coprolites are not uncommon in
384 the fossil record and provide unique palaeoenvironmental-palaeoecological data (Qvarnström
385 et al. 2016, 2017, 2021 and references therein). In the past few years, the non-destructive
386 synchrotron microtomography technique has proven to be quite useful to identify dung beetle
387 elements within coprolites (Qvarnström et al. 2021 and references therein). As already
388 mentioned, non-destructive techniques have not been utilized in the present investigation to
389 identify biotic inclusions within Lotkheri coprolites and hint at the scope of future
390 investigations on Mesozoic-Cenozoic coprolite material from India. However, it is generally
391 agreed that the presence of burrow and/or egg-like structures within coprolites linked to dung
392 beetle are suggestive of the prevalence of a terrestrial palaeoenvironment. Associated faunal
393 remains support that the Lotkheri coprolites were deposited in a palustrine/lacustrine fresh to
394 brackish water environment.

395 Rare occurrences of external markings on coprolites such as feeding traces or tooth
396 impressions have been recorded in the published literature that has been linked to tiger sharks
397 (e.g., genus *Galeocerdo*) or gar fishes (e.g., genus *Lepisosteus*) (refer to Figs. 3I, 5I in
398 Månsby 2009; Fig. 2A in Godfrey & Smith 2010; Figs. 1-3 in Godfrey & Palmer 2015).

399 Bite marks are observed on the external surface of a few Lotkheri coprolite specimens
400 assigned to morphotype M2 (Figs. 2g, 2i1). The glancing bite approximately 2 cm in length
401 (Fig. 2g) is identical to the one assigned to the garfish genus *Lepisosteus* by Godfrey &
402 Palmer (2015) while smaller (<5 mm length) 3-paired (nearly conjoined at one end) troughs
403 (Fig. 2i1) are identical to the one recorded by these workers but assigned to an unknown
404 animal. Interestingly, fish scales belonging to *Lepisosteus indicus* (Figs. 4n-p) were also
405 recovered in association with the coprolite assemblage recorded herein and argues in favour
406 of the glancing bite produced by this fish during coprophagy.

407 The phosphatic composition of the coprolites recorded herein is confirmed by utilizing
408 scanning electron microscopy and geochemical data. Interestingly, the Hydroxyapatite (HAP)
409 crystals observed as inclusions depict three distinct morphologies: spherical (HAP-S), rod-
410 like (HAP-R), and needle-like (HAP-N). We envisage that the freshly excreted faecal matter
411 that consisted of an ionic aqueous solution containing different ions such as Ca^{2+} , PO_4^{3-} , OH^- ,
412 and H^+ help explain the formation of these varied types of phosphatic crystals (Fig10). The
413 growth unit model as shown in Fig. 10 postulates that the presence of Ca^{2+} , PO_4^{3-} , and
414 H^+/OH^- ions in newly expelled faeces constitutes the growth unit, and the pH regulates the
415 concentration of both positively and negatively charged growth units. Neutral conditions are
416 crucial for the concentration of positive and negative growth units to balance, leading to the
417 crystallization and maturation of HAP crystals through various morphologies. A pH of
418 around 7-8 in the post-depositional environment remineralizes faeces into HAP, which is the
419 least soluble phase formed under neutral or basic conditions. Overall, calcium phosphate in
420 coprolite is a result of both precipitation and adsorption processes, where minerals from the
421 surrounding soil or water can deposit on its surface or adsorb onto it. The crystalline
422 structures, intermediate forms, and amorphous aggregates of calcium phosphate in coprolites
423 provide valuable information about the organism's gut and the events that influenced calcium

424 phosphate precipitation before, during, and after its formation. Additionally, organic matter in
425 faeces can serve as a template for calcium phosphate precipitation, affecting its development.
426 The remineralisation of calcium phosphate is dependent on various factors, including pH,
427 concentration, temperature changes, and metabolic processes.

428 **CONCLUSIONS**

429 A detailed account of reptilian coprolites from the Maastrichtian intertrappean deposit of
430 Lotkheri (central India) reveals the presence of five morphotypes i.e., spherical-M1, tear-drop
431 shaped-M2, elliptical-M3, cylindrical-M4 and irregularly folded-M5. The common presence
432 of undigested bone matter and plant remains within morphotypes M1, M2, and M3 supports
433 an omnivorous diet of the producer most likely chelonians. Absence of bone inclusions
434 within morphotype M4 hints at a producer having an effective digestive system most likely a
435 crocodylian. The occurrence of chelonian (mainly scutes) and crocodylian (scutes and teeth)
436 remains in association with coprolites (recorded herein) supports the proposed reptilian
437 producer associations. Scanning electron microscopy and geochemical data confirms the
438 phosphatic composition of the reptilian coprolites investigated herein. Hydroxyapatite
439 crystals (as inclusions) showcase three distinct morphologies i.e., spherical, rod-shaped, and
440 needles. The proposed chemical model envisages that the freshly excreted faecal matter
441 consisting of an ionic aqueous solution containing different ions such as Ca^{2+} , PO_4^{3-} , OH^- , and
442 H^+ explains the formation of these varied types of phosphatic crystals. The external surface of
443 morphotype 2 coprolites provides rare evidence of two different types of bite marks herein
444 linked to garfish *Lepisosteus* and to an unknown animal practising coprophagy. Data on
445 inclusions (both biotic and abiotic), and associated vertebrate remains indicate that the
446 recorded coprolite ichnofossils were deposited in a palustrine/lacustrine fresh to brackish
447 water palaeoenvironment.

448

449 **ACKNOWLEDGEMENTS**

450 The authors are thankful to the Director (BSIP, Lucknow) for providing the necessary
451 infrastructure, encouragement, and permission(s) to carry out this investigation...

452 **REFERENCES**

- 453 Amstutz, G. C. (1958). Coprolites: a review of the literature and a study of specimens from
454 southern Washington. *Journal of sedimentary research*, 28(4), 498–508.
- 455 Bajdek, P., and Bienkowska-Wasiluk, M. (2020). Deep-sea ecosystem revealed by teleost
456 fish coprolites from the Oligocene of Poland. *Palaeogeography Palaeoclimatology
457 Palaeoecology*, 540, 109546. <https://doi.org/10.1016/j.palaeo.2019.109546>.
- 458 Bajdek, P., Qvarnström, M., Qwocki, K., Sulej, T., Sennikov, A.G., Golubev, V.K.,
459 &Niedźwiedzki, G. (2016). Microbiota and food residues including possible evidence
460 of premammalian hair in Upper Permian coprolites from Russia. *Lethaia*, 49, 455–477.
461 <https://doi.org/10.1111/let.12156>
- 462 Balaguera-Reina, S. A., Venegas-Anaya, M., Beltrán-López, V., Cristancho, A., &Densmore
463 III, I. D. (2018). Food habits and ontogenetic dietary partitioning of American
464 crocodiles in a tropical pacific island in central America. *Ecosphere*, 9(9),
465 e02393.10.1002/ecs2.2393.
- 466 Barrios-de Pedro, S., Poyato-Ariza, F.J., Moratalla, J.J., &Buscalioni, Á.D. (2018).
467 Exceptional coprolite association from the early cretaceous continental Lagerstätte of
468 Las Hoyas, Cuenca, Spain. *PloS One*, 13, e0196982.
469 <https://doi.org/10.1371/journal.pone.0196982>.
- 470 Brachaniec, T., Niedźwiedzki, R., Surmik, D., Krzykowski, T., Szopa, K., Gorzelak,
471 P.,&Salamon, M.A. (2015). Coprolites of marine vertebrate predators from the lower
472 Triassic of southern Poland. *Palaeogeography Palaeoclimatology Palaeoecology*, 435,
473 118–126. <https://doi.org/10.1016/j.palaeo.2015.06.005>.
- 474 Brachaniec, T., &Wieczorek, A. (2016). Possible vertebrate coprolites from the upper
475 cretaceous (coniacian) of the sudetes mountains (southern Poland). *Carnets de
476 Géologie*, 16, 349–354. <https://doi.org/10.4267/2042/60665>.
- 477 Broughton, P., Simpson, F., &Whitaker, S. (1978). Late cretaceous coprolites from western
478 Canada. *Palaeontology*, 21, 443–453.
- 479 Chin, K. (2002). Analyses of coprolites produced by carnivorous vertebrates. *The
480 Paleontological Society Papers*, 8, 43–50.
481 <https://doi.org/10.1017/s1089332600001042>.
- 482 Chin, K., Feldmann, R.M., &Tashman, J.N. (2017). Consumption of crustaceans by
483 megaherbivorous dinosaurs: dietary flexibility and dinosaur life history strategies.
484 *ScientificReports*, 7, 11163. <https://doi.org/10.1038/s41598-017-11538-w>.
- 485 Chin, K., &Gill, B.D. (1996). Dinosaurs, dung beetles, and conifers: participants in a
486 cretaceous food web. *Palaios*, 11(3), 280–285.
- 487 Coulson, R. A., Herbert, J.D., &Coulson, T.D. (1989). Biochemistry and physiology of
488 alligator metabolism in vivo. *American Zoologist*, 29(3), 921–934.
- 489 Dentzien-Dias, P., Carrillo-Briceño, J.D., Francischini, H., & Sánchez, R. (2018).
490 Paleocological and taphonomical aspects of the late Miocene vertebrate coprolites
491 (Urumaco formation) of Venezuela. *Palaeogeography Palaeoclimatology
492 Palaeoecology*, 490, 590–603. <https://doi.org/10.1016/j.palaeo.2017.11.048>.

- 493 Fantasia, A., Adatte, T., Spangenberg, J.E., & Font, E. (2016). Palaeoenvironmental changes
494 associated with deccan volcanism, examples from terrestrial deposits from central
495 India. *Palaeogeography Palaeoclimatology Palaeoecology*, 441, 165–180.
496 <https://doi.org/10.1016/j.palaeo.2015.06.032>.
- 497 Gates-Rector, S., & Blanton, T. (2019). The powder diffraction file: a quality materials
498 characterisation database. *Powder Diffraction*, 32(4), 352–360.
- 499 Godfrey, S., & Palmer, B. (2015). Gar-bitten coprolite from South Carolina, USA. *Ichnos*, 22,
500 103–108.
- 501 Godfrey, S., & Smith, J.B. (2010). Shark bitten vertebrate coprolites from the Miocene of
502 Maryland. *Naturwissenschaften*, 97, 461–467.
- 503 Hansen, B., Milan, J., Clemmensen, L., Adolfsen, J., Estrup, E., Klein, N., Mateus, O.,
504 & Wings, O. (2015). Coprolites from the late Triassic KapStewart Formation, Jameson
505 Land, East Greenland: morphology, classification and prey inclusions. *Geological*
506 *Society, London, Special Publications*, 434. <http://doi.org/10.1144/sp434.12>.
- 507 Häntzschel, W., El-Baz, F., & Amstutz, G.C. (1968). Coprolites: an annotated bibliography.
508 *Memoirs of the Geological Society of America*, 108, 1–132.
- 509 Hollocher, K.T., Hollocher, T.C., & Rigby, J.K. (2010). A phosphatic coprolite lacking
510 diagenetic permineralization from the Upper Cretaceous Hell Creek Formation,
511 northeastern Montana: importance of dietary calcium phosphate in preservation.
512 *Palaios*, 25, 132–140. <https://doi.org/10.2110/palo.2008.p08-132r>.
- 513 Hunt A.P., Lucas S.G., & Spielmann J.A. (2012). The vertebrate coprolite collection at the
514 Natural History Museum (London). In A.P. Hunt, J. Milàn, S.G. Lucas, & J.A.
515 Spielmann (Eds.), *Vertebrate Coprolites: New Mexico Museum of Natural History and*
516 *Science Bulletin*, 57, 125–130.
- 517 Hunt, A., Lucas, S.G., Milàn, J., Lichtig, A.J., & Jagt, J.W.M. (2015). Vertebrate coprolites
518 from cretaceous chalk in Europe and north America and the shark surplus paradox.
519 In R.M. Sullivan & S.G. Lucas (Eds.), *Fossil record 4: New Mexico Museum of Natural*
520 *History and Science Bulletin*, 67, 63–68.
- 521 Jensen, K., & Das, I. (2008). Cultural exploitation of freshwater turtles in Sarawak,
522 Malaysian Borneo. *Chelonian conservation biology*, 7, 281–285.
523 <https://doi.org/10.2744/ccb-0657.1>.
- 524 Kapur, V.V., Bajpai, S., Sarvanan, N., & Das, D.P. (2006). Vertebrate fauna from Deccan
525 intertrappean beds of Bhanpura, Mandsaur District, Madhya Pradesh. *Gondwana*
526 *Geological Magazine*, 21, 43–46.
- 527 Kapur, V.V., & Khosla, A. (2019). Faunal elements from the deccan volcano-sedimentary
528 sequences of India: a reappraisal of biostratigraphic, palaeoecologic, and
529 palaeobiogeographic aspects. *Geological journal*, 54, 2797–2828.
530 <https://doi.org/10.1002/gj.3379>.
- 531 Kapur, V.V., Kumar, K., Morthekai, P., & Chaddha, A.S. 2020. Palaeodiet of Miocene
532 producers and depositional environments: inferences from the first evidence of
533 microcoprolites from India. *Acta Geologica Sinica – English Edition*, 94, 1574–1590.
534 <https://doi.org/10.1111/1755-6724.14293>.
- 535 Keller, G., Paula, M., Johannes, M., Nicolas, T., Jahanavi, P., Jorge, S., Sigal, A., & Sarit,
536 A.P. (2020). Mercury linked to deccan trap volcanism, climate change and the end-
537 Cretaceous mass extinction. *Global and Planetary change*, 194,
538 103312. <https://doi.org/10.1016/j.gloplacha.2020.103312>.
- 539 Khosla, A., Chin, K., Alimohammadin, H., & Dutta, D. (2015). Ostracods, plant tissues, and
540 other inclusions in coprolites from the late Cretaceous Lameta Formation at Pisdura,
541 India: taphonomical and palaeoecological implications. *Palaeogeography*
542 *Palaeoclimatology Palaeoecology*, 418, 90–100.

- 543 <https://doi.org/10.1016/j.palaeo.2014.11.003>.
- 544 Lamboy, M., Purnachandrarao, V., Ahmed, E., &Azzouzi, N. (1994). Nanostructure and
545 significance of fish coprolites in phosphorites. *Marine Geology*, *120*, 373–383.
- 546 Lucas, S.G., Spielmann, J.A., Hunt, A.P., &Emry, R.J. (2012). Crocodylian coprolites from
547 the Eocene of the ZaysanBasin, Kazakstan. In A.P. Hunt, J. Milàn, S.G. Lucas, &J.A.
548 Spielmann (Eds.), *Vertebrate Coprolites: New Mexico Museum of Natural History and*
549 *Science Bulletin*, *57*, 319–324.
- 550 Matley, C.A. (1939). The coprolites of Pisdura, central province. *Records of the Geological*
551 *Survey of India*, *74*, 535–547.
- 552 Månsby, U. (2009). Late cretaceous coprolites from the Kristianstad Basin, southern Sweden.
553 Unpublished Bachelor Thesis, Department of Geology, Lund University, 16 pp.
- 554 Milàn, J.(2012). Crocodylian scatology – a look into morphology, internal architecture, inter-
555 and intraspecific variation and prey remains in extant crocodylian feces. In A.P. Hunt,
556 J. Milàn, S.G. Lucas, &J.A. Spielmann (Eds.), *Vertebrate Coprolites: New Mexico*
557 *Museum of Natural History and Science Bulletin*, *57*, pp. 65–72.
- 558 Milàn, J., Hunt, A., Adolfssen, J., Rasmussen, B., and Bjerager, M. (2015). First record of a
559 vertebrate coprolite from the Upper Cretaceous (Maastrichtian) Chalk of StevnsKlint,
560 Denmark. In R.M. Sullivan& S.G. Lucas (Eds.), *Fossil record 4: New Mexico Museum*
561 *of Natural History and Science Bulletin*, *67*, 227–230.
- 562 Muftah, A.M., El-Shawaihdi, M.H., Al Riay, M.H., &Boaz, N.T.(2020). Coprolites from the
563 Neogene Sahabi Formation, northeasternSirtBasin of Libya. *Arabian Journal of*
564 *Geosciences*, *13*, 223. <https://doi.org/10.1007/s12517-020-5219-x>.
- 565 Nobre, P. H., De Souza Carvalho, I., De Vasconcellos, F. M., &Souto, P. R. (2008). Feeding
566 behavior of the gondwaniccrocodylomorpha*Mariliasuchusamarali* from the Upper
567 Cretaceous Bauru Basin, Brazil. *Gondwana Research*, *13*, 139–
568 145.<https://doi.org/10.1016/j.gr.2007.08.002>.
- 569 Northwood, C. (2005). Early Triassic coprolites from Australia and their
570 palaeobiologicalsignificance. *Palaeontology*, *48*, 49–68.
571 <https://doi.org/10.1111/j.1475-4983.2004.00432.x>.
- 572 Owocki, K., Niedzwiedzki, G., Sennikov, A.G., Golubev, V.K., Janiszewska, K., &Sulej, T.
573 (2013). Upper Permian vertebrate coprolites from Vyazniki and Gorokhovets, Vyatkian
574 regional Stage, Russian platform. *Palaios*, *27*, 867–877.
575 <https://doi.org/10.2110/palo.2012.p12-017r>.
- 576 Pande, K. (2002). Age and duration of the deccan traps, India: a review of radiometric and
577 paleomagnetic constraints. *Journal of Earth System Science*, *111*, 115–123.
- 578 Prasad, V., Strömberg, C.A.E., Alimohammadian, H., & Sahni, A. (2005). Dinosaur
579 coprolites and the early evolution of grasses and grazers. *Science*, *310*, 1177–1180.
580 <https://doi.org/10.1126/science.1118806>.
- 581 Purnachandrarao, V., & Lamboy, M. (1995). Phosphorites from the Oman margin, ODP leg
582 117. *OceanologicaActa*, *18*, 289–307.
- 583 Qvarnström, M., Niedzwiedzki, G., &Žigaite, Ž.(2016). Vertebrate coprolites (fossilized
584 faeces): an unexplored Konservat-Lagersätte. *Earth Science Reviews*, *162*, 44–57.
- 585 Qvarnström, M., Niedzwiedzki, G., Tafforeau, P., Žigaite, Ž., &Ahlberg, P.E. 2017.
586 Synchrotron phase-contrast microtomography of coprolites generates novel
587 palaeobiological data. *Scientific Reports*, *7*, 2723. [https://doi.org/10.1038/s41598-017-](https://doi.org/10.1038/s41598-017-02893-9)
588 [02893-9](https://doi.org/10.1038/s41598-017-02893-9).
- 589 Qvarnström, M., Fikáček, M., Wernström, J.V., Huld, S., Beutel, R.G., Arriaga-Varela, E.,
590 Ahlberg, P.E., &Niedzwiedzki, G.(2021). Exceptionally preserved beetles in a Triassic
591 coprolite of putative dinosauriform origin. *Current Biology*, *31*, 3374–3381.

- 592 Richter, G., &Baszio, S. (2001a). Traces of a limnic food web in the Eocene Lake Messel —
593 a preliminary report based on fish coprolite analyses. *Palaeogeography*
594 *Palaeoclimatology Palaeoecology*, 166, 345–368. <https://doi.org/10.1016/s0031->
595 0182(00)00218-2.
- 596 Richter, G., &Baszio, S. (2001b). First proof of planctivory/insectivory in a fossil fish:
597 *Thaumaturus intermedius* from the Eocene Lake Messel (FRG). *Palaeogeography*
598 *Palaeoclimatology Palaeoecology*, 173, 75–85.
599 [https://doi.org/10.1016/s0031-0182\(01\)00318-2](https://doi.org/10.1016/s0031-0182(01)00318-2).
- 600 Rummy, P., Halaclar, K., & Chen, H.(2021). The first record of exceptionally-preserved
601 spiral coprolites from the Tsagan-TsabFormation (Lower Cretaceous), Tatal, western
602 Mongolia. *Scientific Reports*, 11, 7891. <https://doi.org/10.1038/s41598-021-87090-5>.
- 603 Sagar, R., Kapur, V.V., Kumar, K., Morthekai, P., Sharma, A., Shukla, S., Ghosh, A.K.,
604 Chauhan, G., & Thakkar, M.G. (2022). The first record on cm-sized vertebrate
605 coprolites from the early-middle Miocene (Aquitania-Langhian) Khari Nadi and
606 Chassra formations, Kutch Basin, western India: palaeobiological significance. *Pre-*
607 *print SSRN electronic journal*. DOI: 10.2139/ssrn.4269941.
- 608 Sahni, A., &Mishra, V.P.(1975). Lower tertiary vertebrates from western India. *Monographs*
609 *of the Palaeontological Society of India*, 3, 1–48.
- 610 Schoene, B., Samperton, K.M., Eddy, M.P., Keller, G., Adatte, T., Bowring, S.A., Khadri,
611 S.F.R., &Gertsch, B.(2015). U-pb geochronology of the deccan traps and relation to the
612 end-Cretaceous mass extinction. *Science*, 347(6218), 182–
613 184. <https://doi.org/10.1126/science.aaa0118>.
- 614 Schwimmer, D., Weems, R., & Sanders, A. (2015). A late Cretaceous shark coprolite with
615 baby freshwater turtle vertebrae inclusions. *Palaios*, 30, 707–713. DOI:
616 10.2110/palo.2015.019.
- 617 Segesdi, M., Botfalvai, G., Bodor, E., Ósi, A., Buczkó, K., Dallos, Z., Tokai, R., &Földes, T.
618 (2017). First report on vertebrate coprolites from the upper cretaceous (Santonian)
619 CsehbányaFormation of Iharkút, Hungary. *Cretaceous Research*, 74, 87–
620 99. <https://doi.org/10.1016/j.cretres.2017.02.010>.
- 621 Self, S., Jay, A., Widdowson, M., &Keszthelyi, L. (2008). Correlation of the deccan and
622 Rajahmundry trap lavas: are these the longest and largest lava flows on earth?. *Journal*
623 *of Volcanology and Geothermal Research*, 172, 3–19.
624 <https://doi.org/10.1016/j.jvolgeores.2006.11.012>.
- 625 Sharma, M.K., & Patnaik, R. (2010). Coprolites from the lower Miocene Baripada beds of
626 Orissa. *Current Science*, 99, 804–808.
- 627 Souto, P.R.F. (2010). Crocodylomorph coprolites from the Bauru basin, Upper Cretaceous,
628 Brazil. *New Mexico Museum of Natural History and Science Bulletin*, 51, 201– 208.
- 629 Suazo, T.L., Cantrell, A.K, Lucas, S.G., Spielmann, J.A, & Hunt, A.P. (2012). Coprolites
630 acrossCretaceous/Tertiary Boundary, San Juan Basin. In A.P. Hunt, J. Milàn, S.G.
631 Lucas, &J.A. Spielmann (Eds.), *Vertebrate Coprolites: New Mexico Museum of*
632 *Natural History and Science Bulletin*, 57,263–274.
- 633 Sullivan, R., &Jasinski, S. (2012). Coprolites from the Upper Cretaceous Fruitland, Kirtland
634 and Ojo Alamo formations, San Juan Basin, New Mexico. In A.P. Hunt, J. Milàn, S.G.
635 Lucas, &J.A. Spielmann (Eds.), *Vertebrate Coprolites: New Mexico Museum of*
636 *Natural History and Science Bulletin*, 57, 255–262.
- 637 Trutnau, L. &Sommerlad, R. (2006). Crocodylians. Their natural history & captive
638 husbandry, first ed. Chimaera, Frankfurt, Germany, 308–354 pp.
- 639 Vajda, V., Pesquero Fernández, M.D., Villanueva-Amadoz, U., Lehsten, V., andAlcalá,
640 L.(2016). Dietary and environmental implications of early cretaceous predatory

641 dinosaur coprolites from Teruel, Spain. *Palaeogeography Palaeoclimatology*
642 *Palaeoecology*, 464, 134–142. <https://doi.org/10.1016/j.palaeo.2016.02.036>.

643 Waldman, M. (1970). Comments on a cretaceous coprolite from Alberta, Canada. *Canadian*
644 *Journal of Earth Sciences*, 7, 1008–1012.

645 Yao, M., Sun, Z., Meng, Q., Li, J., & Jiang, D. (2022). Vertebrate coprolites from middle
646 Triassic Chang 7 Member in Ordos Basin, China: palaeobiological and
647 palaeoecological implications. *Palaeogeography Palaeoclimatology Palaeoecology*,
648 600, 111084. <https://doi.org/10.1016/j.palaeo.2022.111084>.

649 Zatoń, M., Niedźwiedzki, G., Marynowski, L., Benzerara, K., Pott, C., Cosmidis, J.,
650 Krzykowski, T., & Filipiak, P. (2015). Coprolites of late Triassic carnivorous vertebrates
651 from Poland: an integrative approach. *Palaeogeography Palaeoclimatology*
652 *Palaeoecology*, 430, 21–46. <https://doi.org/10.1016/j.palaeo.2015.04.009>.

653
654

655

656

657

658

659

660

661

662

663

664

665

666

667

668

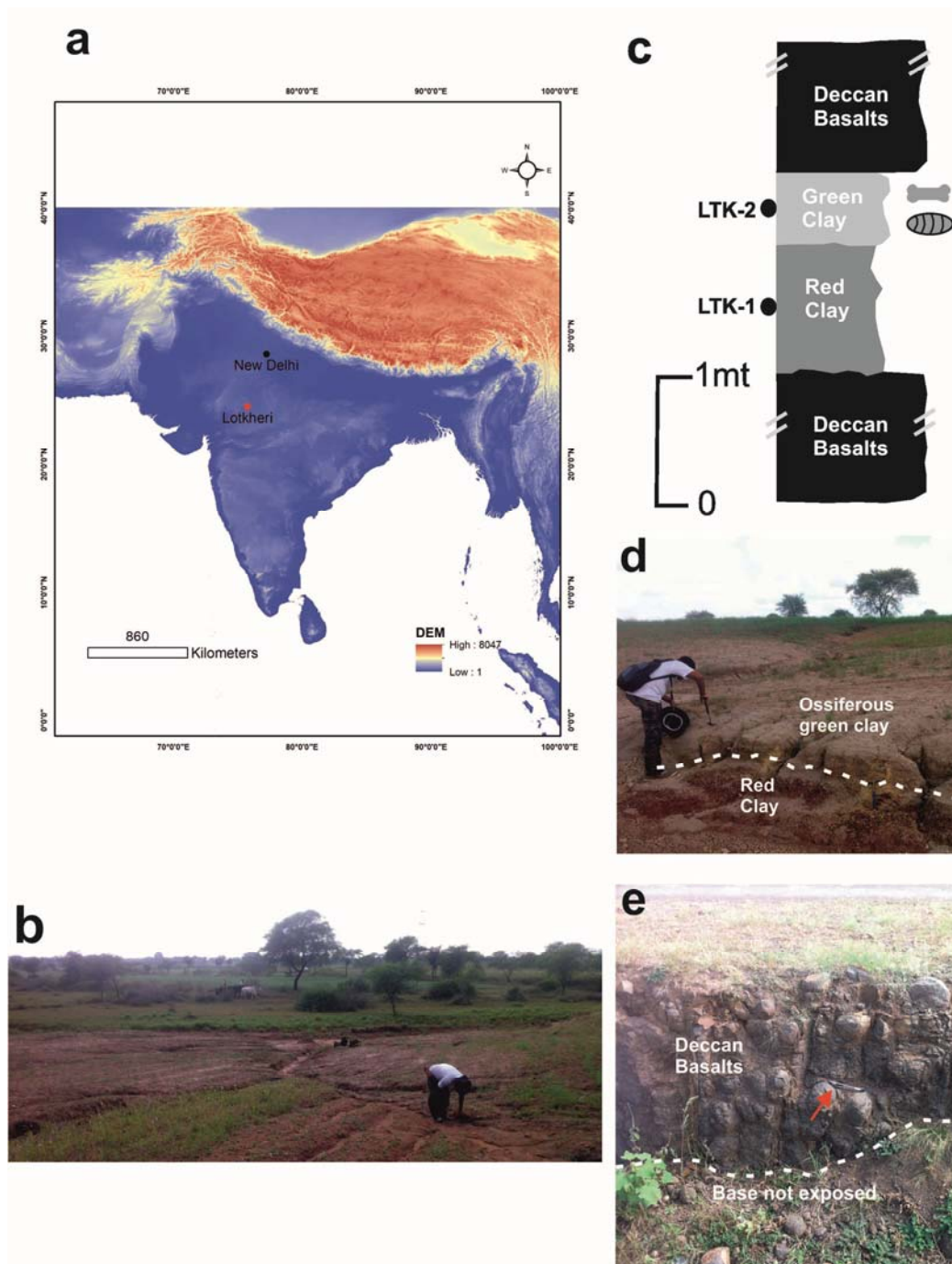
669

670

671

672

673 **EXPLANATION OF FIGURES**

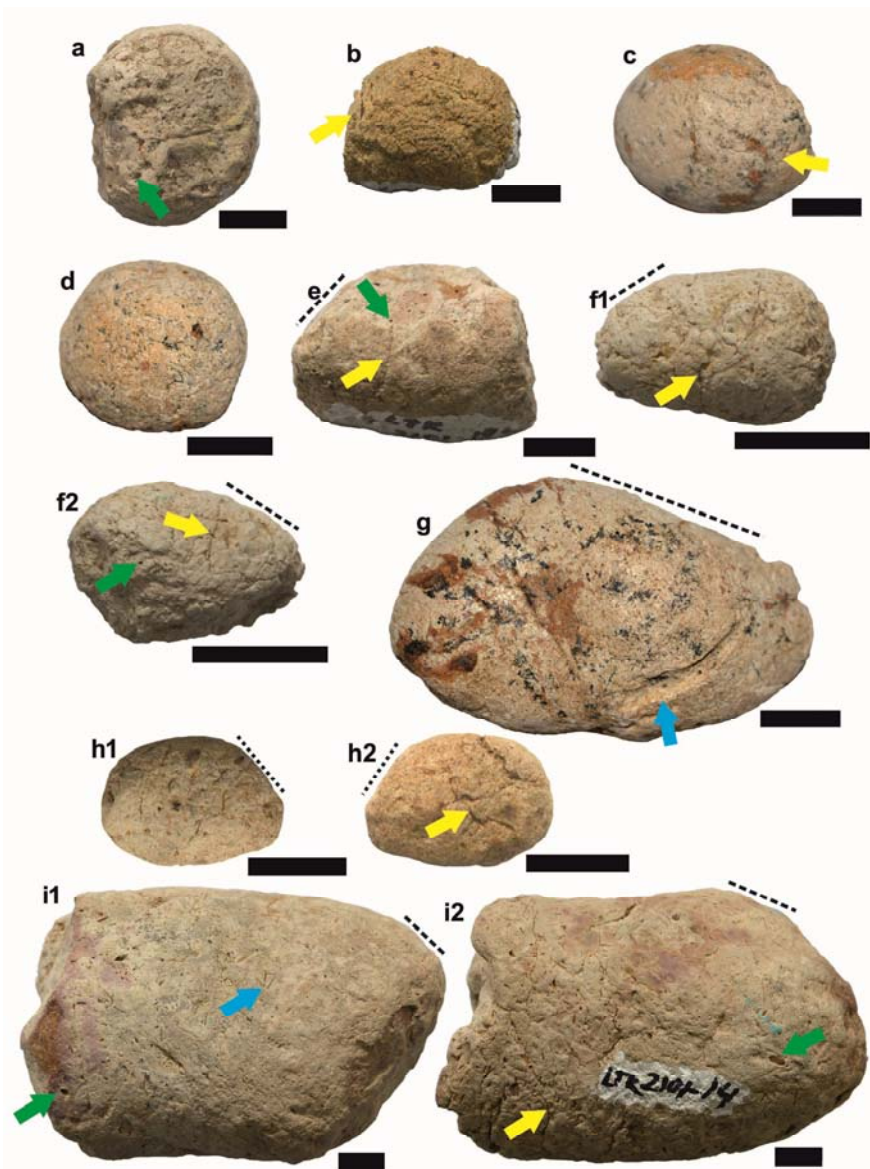


674

675

676 **Fig. 1.** (a) DEM map showing location of the investigated late Cretaceous (Maastrichtian) locale of Lotkheri in
677 central India. (b) Panoramic view of the Lotkheri locale while conducting surface prospecting in the ploughed
678 field (farmland) for vertebrate remains and associated coprolites. (c) Lithostratigraphic section. (d) Field
679 photograph showing the contact between fossiliferous (coprolite-yielding) green clays and the underlying
680 unfossiliferous red clays. (e) Exposure of the underlying basalt in a nala section in the vicinity of the coprolite-
681 yielding locale showing spheroidal weathering, red arrow marks a pen for scale purposes.

682



683

684

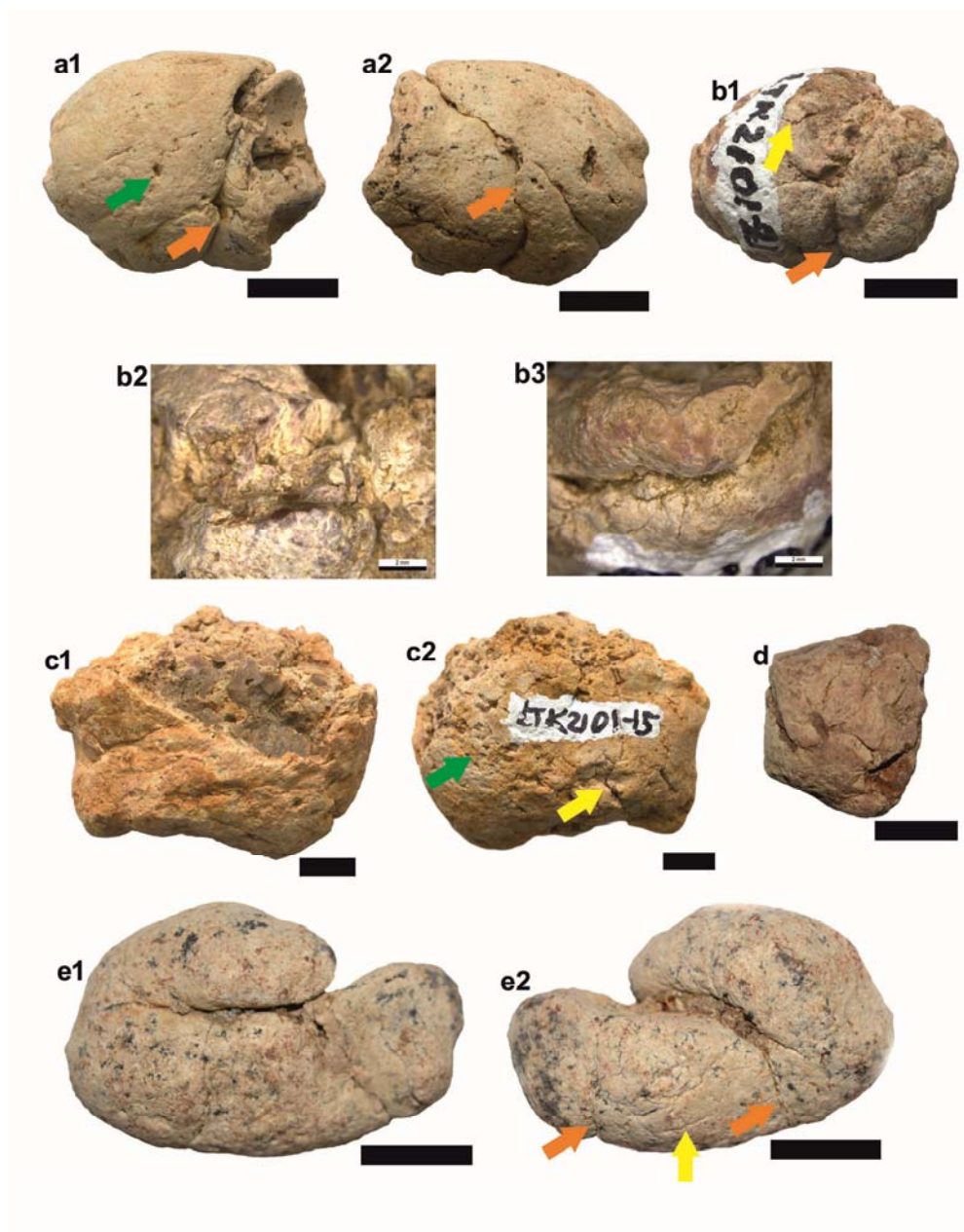
685 **Fig. 2.** Digital photographs of late Cretaceous (Maastrichtian) coprolite specimens recovered from the
686 intertrappean deposit at Lotkheri, central India. (a-d)Spherical Morphotype M1, a. specimen no. LTK/2101-154
687 (BSIP 42254); b. specimen no. LTK/2101-234 (BSIP 42255); c. specimen no. VVK/BNP/GEO2 (BSIP 42256);
688 d. specimen no. VVK/ BNP/GEO1 (BSIP 42253). (e-i)Tear-drop shaped Morphotype M2, e. specimen no.
689 LTK/2101-194 (BSIP 42258); f1-f2. specimen no. LTK/2101-351 (BSIP 42260); g. specimen no.
690 VVK/BNP/GEO12 (BSIP 42257); h1-h2: specimen no. LTK/2101-321 (BSIP 42261); i1-i2. specimen no.
691 LTK/2101-14 (BSIP 42259).Note: Green arrow marks burrow structures, yellow arrow marks desiccation
692 cracks, light blue arrow points towards bite marks, and dashed lines highlight the conspicuous inclination. The
693 scale bar equals 1 cm for all.

694

695

696

697



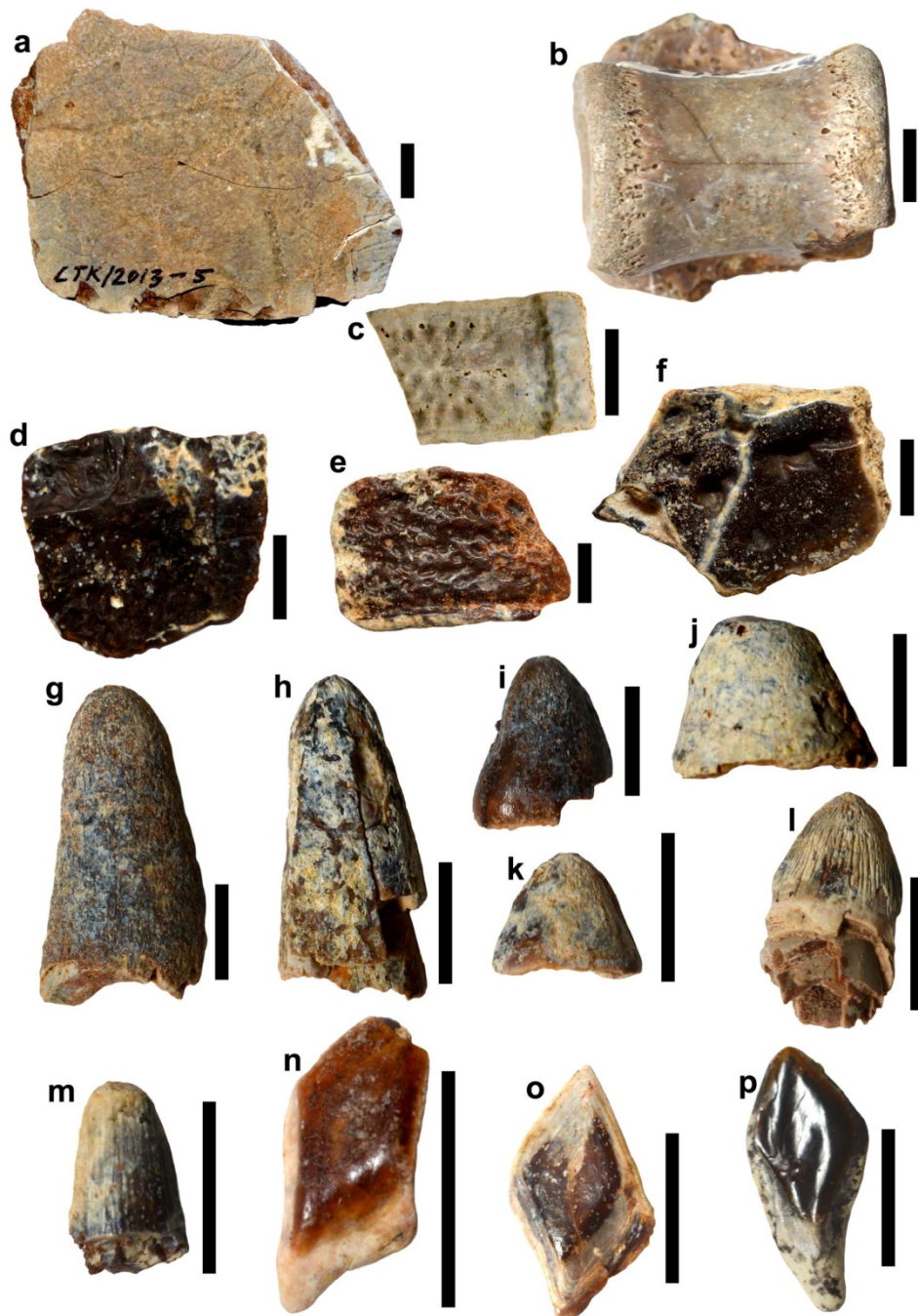
698

699 **Fig.3.** Digital photographs of late Cretaceous (Maastrichtian) coprolite specimens recovered from the
700 intertrappean deposit at Lotkheri, central India. (a-b)Elliptical Morphotype M3,a1-a2. specimen no. LTK/2101-
701 88 (BSIP 42262), b1-b3. specimen no. LTK/2101-21 (BSIP 42263). (c-d)Cylindrical Morphotype M4.[(c1-c2.
702 specimen no. LTK/2101-15 (BSIP 42265);d. specimen no. VVK/BNP/GEO9 (BSIP 42264)]. (e) Irregularly
703 folded Morphotype M5.[(e1-e2. specimen no. VVK/BNP/GEO10 (BSIP 42266)]. Note: b2-b3 are close-up
704 views showing bone matter (reddish pink colour) embedded on the external surface of the coprolite specimen
705 no. LTK/2101-21 (BSIP 42263). The green arrow marks burrow structures, the yellow arrow marks desiccation
706 cracks, and the orange arrow marks constrictions. The scale bar equals 1 cm for all.

707

708

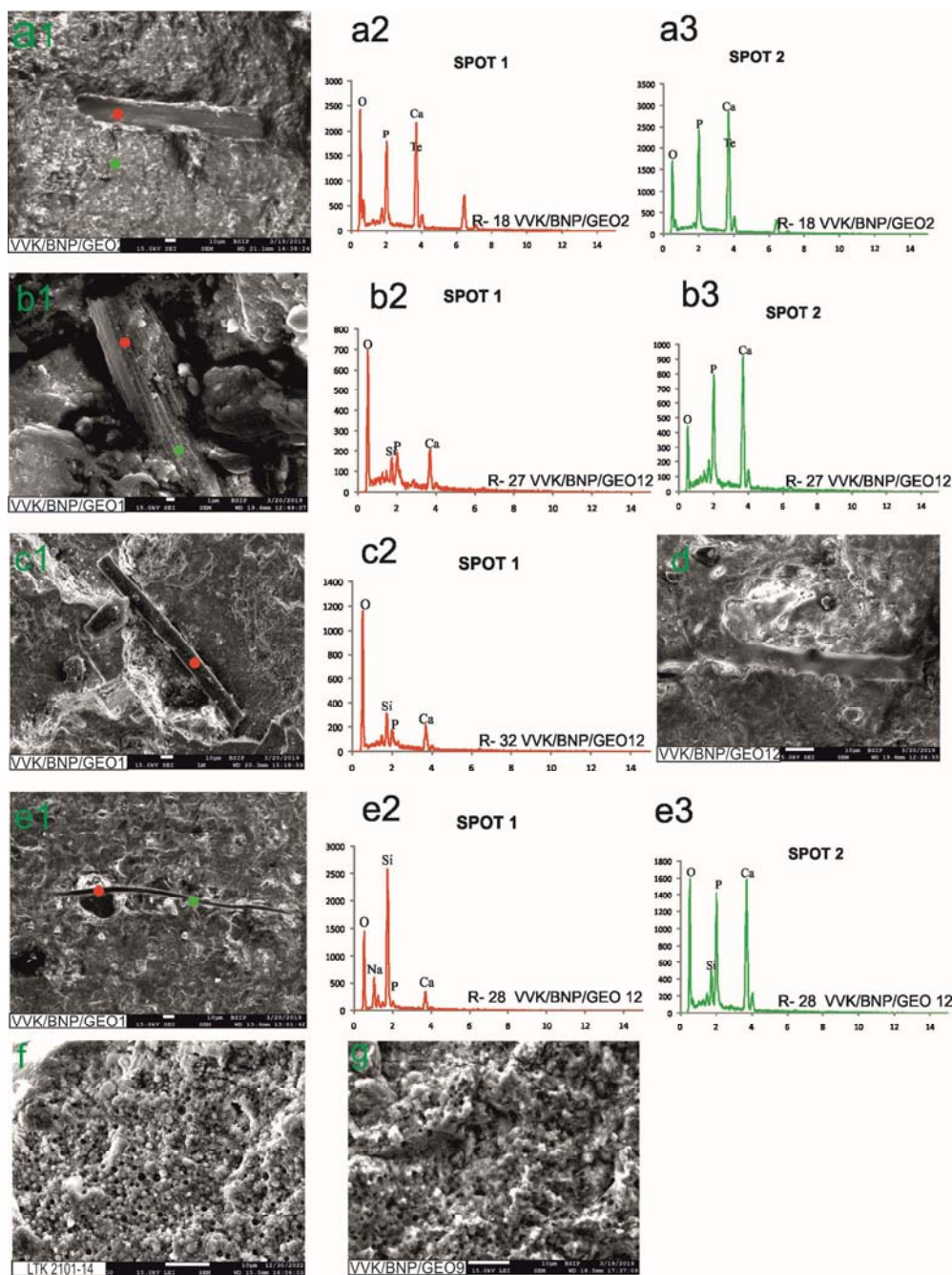
709



710

711 **Fig. 4.** Digital photographs of the late Cretaceous (Maastrichtian) vertebrate remains recovered from the
712 intertrappean deposit at Lotkheri, central India. (a-b) *Chelonia* gen. et sp. indet. (a). carapace fragment,
713 specimen no. LTK/2013-5 (BSIP 42267); (b). isolated vertebra, specimen no. LTK/2101-118 (BSIP 42268). (c-
714 f) dermal scutes, *Crocodylia* gen. et sp. indet. (c. specimen no. LTK/2013-12 (BSIP 42269); d. specimen no.
715 LTK/2013-18 (BSIP 42270); e. specimen no. LTK/2013-1 (BSIP 42271); f. specimen no. LTK/2013-19 (BSIP
716 42272). (g-m) isolated teeth, *Crocodylia* gen. et sp. indet. (g. specimen no. LTK/2013-13 (BSIP 42273); h.
717 specimen no. LTK/2013-11 (BSIP 42274); i. specimen no. LTK/2013-10 (BSIP 42275); j. specimen no.
718 LTK/2013-9 (BSIP 42276); k. specimen no. LTK/2013-16 (BSIP 42277); l. specimen no. LTK/2013-17 (BSIP
719 42278); m. specimen no. LTK/2013-15 (BSIP 42279)). (n-p) isolated scales, *Lepisosteus indicus* (n. specimen no.
720 LTK/2101-266 (BSIP 42280); o. specimen no. LTK/2013-4 (BSIP 42281); p. specimen no. LTK/2013-2 (BSIP
721 42282)). The scale bar equals 1 cm for all.

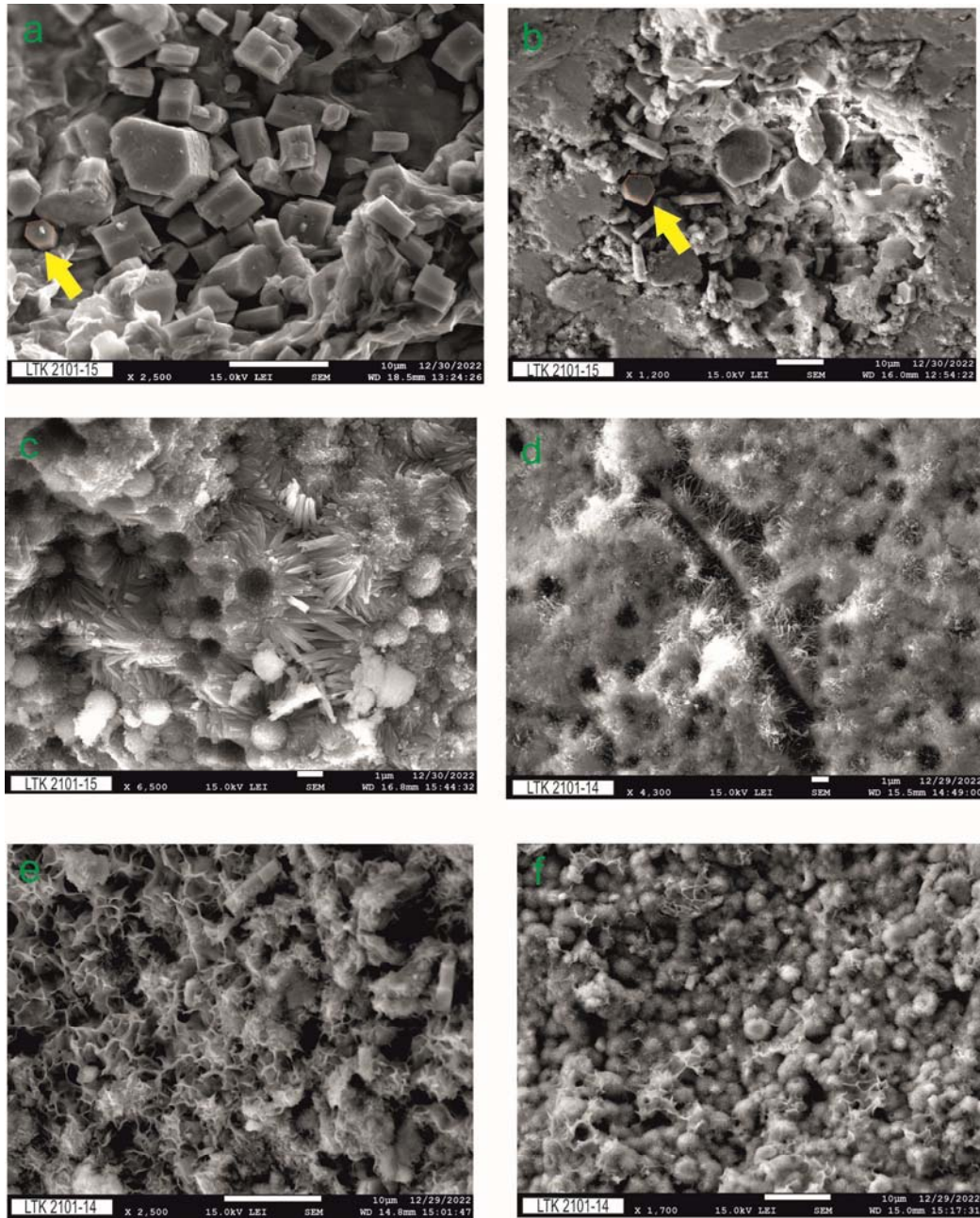
722



723

724 **Fig. 5:** Scanning electron microphotographs showing biotic inclusions and corresponding Energy Dispersive
 725 Spectroscopy (EDS) plots of the late Cretaceous (Maastrichtian) coprolites recovered from the intertrappean
 726 deposit at Lotkheri, central India. (a1-a3). Spherical Morphotype M1, specimen no. VVK/BNP/GEO2 (BSIP
 727 42256), a1. bone fragment, a2. EDS data for spot 1, a3. EDS data for spot 2. (b1-b3) Spherical Morphotype M1,
 728 specimen no. VVK/BNP/GEO1 (BSIP 42253), b1. bone fragment, b2. EDS data for spot 1, b3. EDS data for
 729 spot 2. (c1-c2) Spherical Morphotype M1, specimen no. VVK/BNP/GEO1 (BSIP 42253), c1. bone fragment,
 730 c2. EDS data for spot 1. (d) Tear Drop shaped Morphotype M3, bone fragment, specimen no.
 731 VVK/BNP/GEO12 (BSIP 42257). (e1-e3) Spherical Morphotype M1, specimen no. VVK/BNP/GEO1 (BSIP
 732 42253), e1. Sponge spicule fragment, e2. EDS data for Spot 1, e3. EDS data for Spot 2. (f) Microspherulites
 733 (egg-like mineral spheres), Tear Drop shape Morphotype M2, specimen no. LTK/2101-14 (BSIP 42259). g.
 734 Microspherulites (egg-like mineral spheres), Cylindrical Morphotype M4, specimen no. VVK/BNP/GEO9
 735 (BSIP 42264). For details refer to Supplementary Data S1.

736



737

738 **Fig. 6.** Scanning electron microphotographs showing the internal texture and the Hydroxyapatite (HAP) crystals
739 (as inclusions) within the late Cretaceous (Maastrichtian) coprolites recovered from the intertrapean deposit at
740 Lotkheri, central India. (a-c) Cylindrical Morphotype M4, specimen no. LTK/2101-15 (BSIP 42265). (d-f) Tear
741 Drop shaped Morphotype M3, specimen no. LTK/2101-14 (BSIP 42259). Note: Yellow arrow marks the
742 hexagonal rod-shaped geometry of the HAP crystals. Needle-shaped geometry of the HAP crystals in c & d.
743 Micron-sized spherical geometry of HAP crystals in e & f.

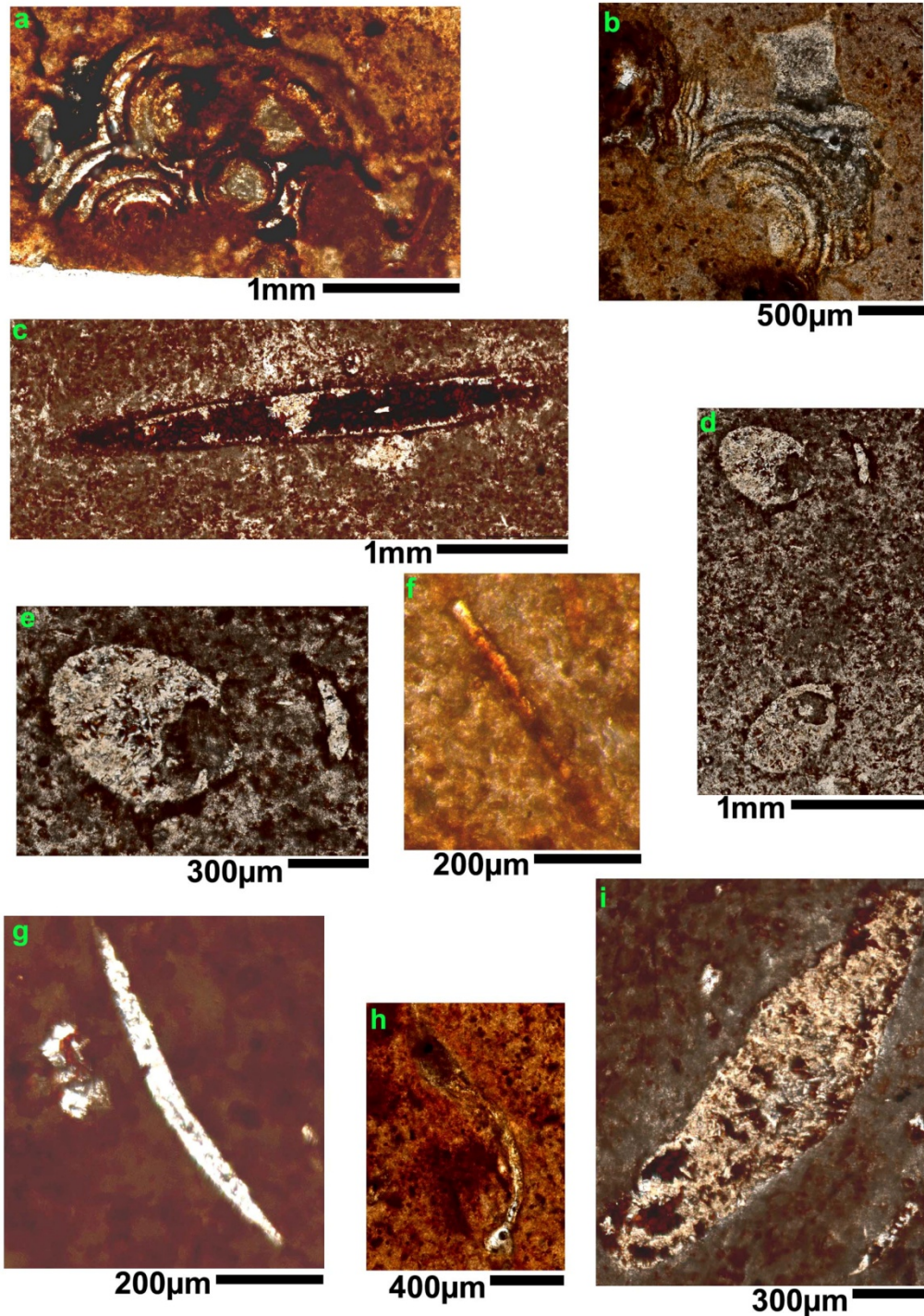
744

745

746

747

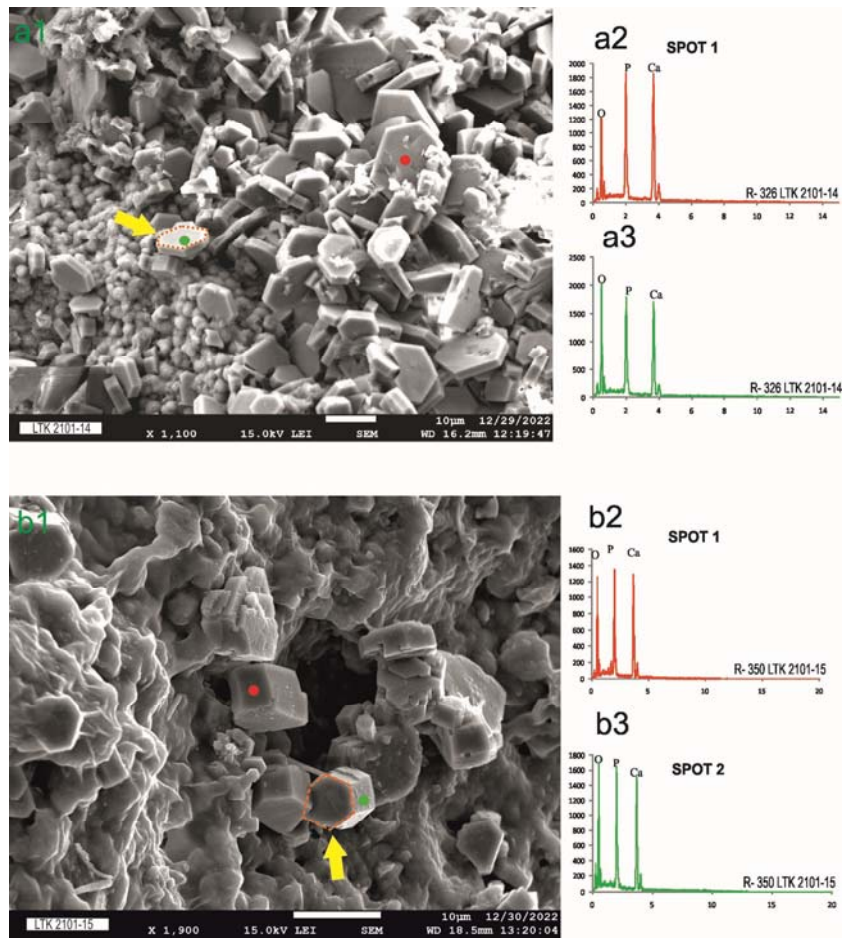
748



749

750 **Fig. 7.** Digital scans of the thin sections showing the biotic inclusions within the late Cretaceous (Maastrichtian)
751 coprolites recovered from the intertrappean deposit at Lotkheri, central India. (a-b) Fish scales, Teardrop-shaped
752 Morphotype M2, specimen no. LTK/2101-14 (BSIP 42259). (c) a cavity or a burrow structure, Cylindrical
753 Morphotype M4, specimen no. LTK/2101-15 (BSIP 42265). (d-e) egg-like structures possibly of a dung beetle,
754 Cylindrical Morphotype M4, specimen no. LTK/2101-15 (BSIP 42265). (f) bone fragment, Teardrop-shaped
755 Morphotype M2, specimen no. LTK/2101-14 (BSIP 42259). (g) freshwater sponge spicule morphotype
756 Acanthoxea, Cylindrical Morphotype M4, specimen no. LTK/2101-15 (BSIP 42265). (h) bone fragment,
757 Teardrop-shaped Morphotype M2, specimen no. LTK/2101-14 (BSIP 42259). (i) burrow structure, Cylindrical
758 Morphotype M4, specimen no. LTK/2101-15 (BSIP 42265).

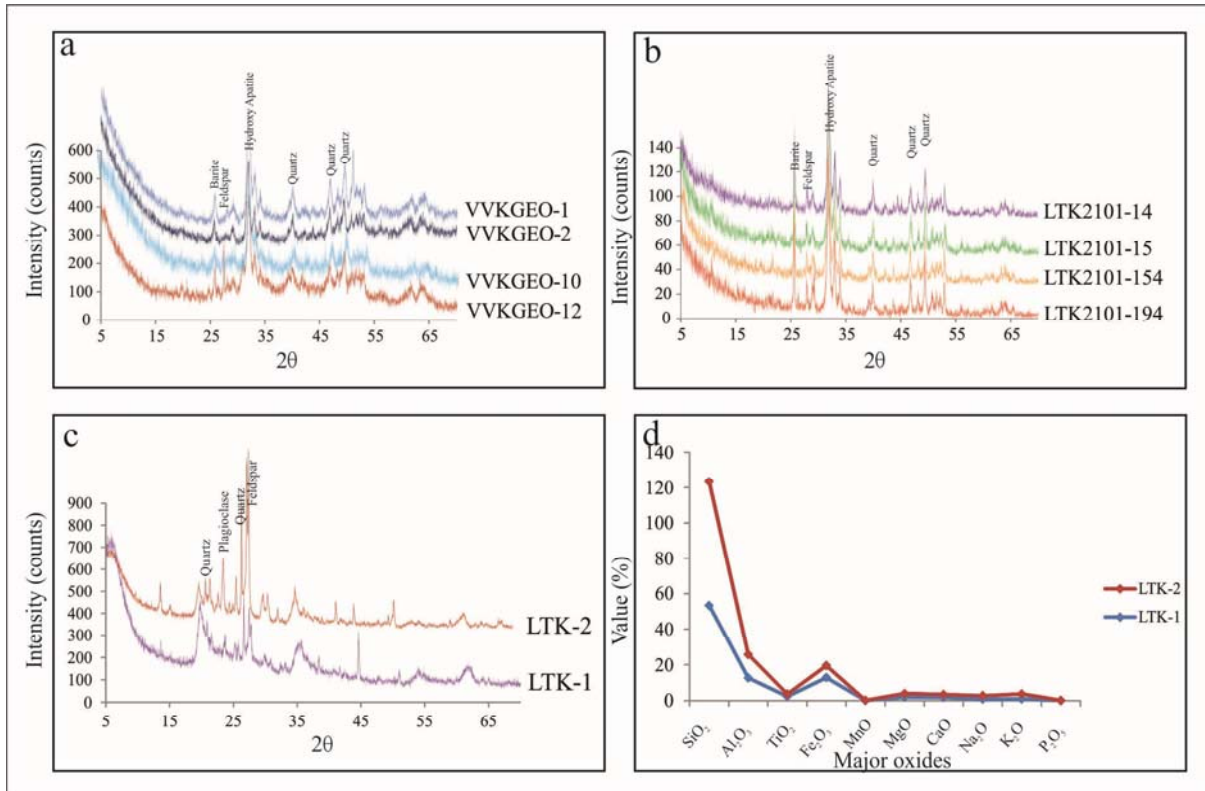
759



760

761 **Fig. 8.** Scanning electron microphotographs showing Hydroxyapatite (HAP) crystals and corresponding Energy
762 Dispersive Spectroscopy (EDS) plots of the late Cretaceous (Maastrichtian) coprolites recovered from the
763 intertrappean deposit at Lotkheri, central India. (a1-a3). Teardrop-shaped Morphotype M2, specimen no.
764 LTK/2101-14 (BSIP 42259), a1. Rod-shaped HAP crystals, a2. EDS data for spot 1, a3. EDS data for spot 2.
765 (b1-b3) Cylindrical Morphotype M4, specimen no. LTK/2101-15 (BSIP 42265), b1. Rod-shaped HAP crystals,
766 b2. EDS data for spot 1, b3. EDS data for spot 2. Note: Yellow arrow marks the hexagonal rod-shaped geometry
767 of HAP crystals.

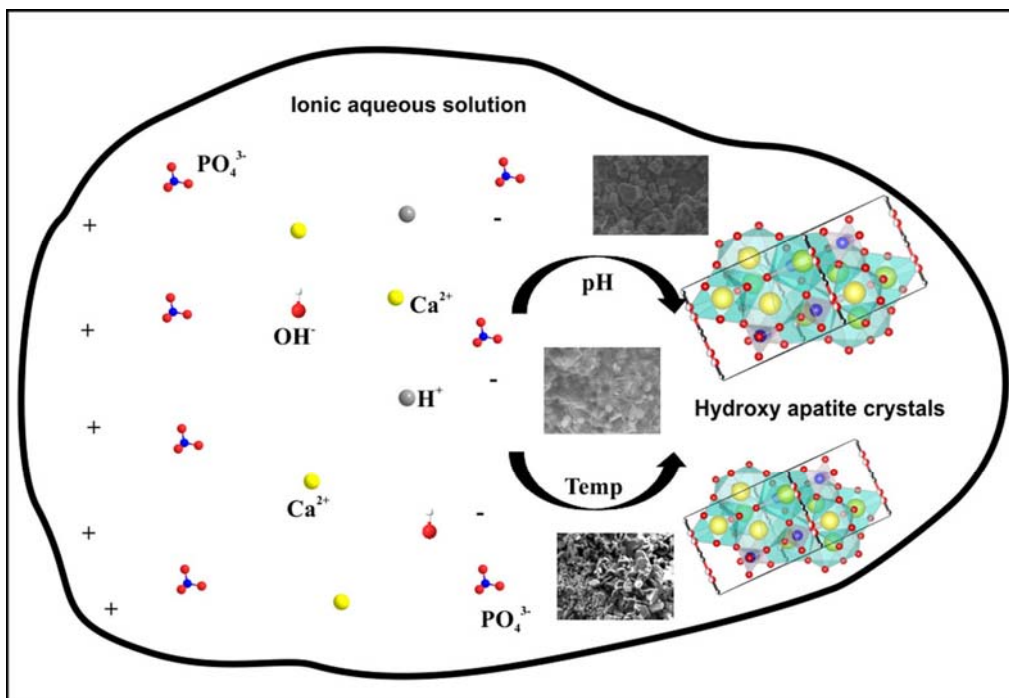
768



769

770 **Fig. 9.** Geochemical data of the late Cretaceous (Maastrichtian) coprolites, associated (LTK-1) and host (LTK-2)
 771 intertrappean sediments from Lotkheri, central India. (a-b) XRD spectra of coprolites. (c) XRD spectra of
 772 associated (LTK-1) and host (LTK-2) lithology. (d) XRF data on major oxides of associated (LTK-1) and host
 773 (LTK-2) lithology.

774



775

776

777

778

779

Fig. 10. Schematic diagram for the Growth Unit Model showing the presence of Ca²⁺, PO₄³⁻, and H⁺/OH⁻ ions
 constituting the growth units that form the three different types i.e., spherical-, rod-, and needle-shaped
 geometry of Hydroxyapatite (HAP) crystals in coprolites.

780 **EXPLANATION OF TABLE**

S. No.	Morphotype(s)	Specimen	Length (in mm)	Width (in mm)	Length/Width	Avg Length (in mm)	Avg.Width (in mm)	Remarks
1	M1 (Spherical)	LTK/2101-154 (BSIP 42254)	30.16	24.18	1.25	26.46	23.17	Fig. 2a
2		LTK/2101-234 (BSIP 42255)	26.78	21.72	1.23			Fig.2b
3		VVK/BNP/GEO2 (BSIP 42256)	20.58	22.35	0.92			Fig. 2c
4		VVK/BNP/GEO1 (BSIP 42253)	28.33	24.44	1.16			Fig. 2d
5	M2 (Teardrop)	LTK/2101-194 (BSIP 42258)	33.44	24.66	1.36	37.97	32.38	Fig. 2e
6		LTK/2101-351 (BSIP 42260)	17.39	11.94	1.46			Fig. 2f1-f2
7		VVK/BNP/GEO12 (BSIP 42257)	33.12	54.37	0.61			Fig. 2g
8		LTK/2101-321 (BSIP 42261)	18.15	13.15	1.38			Fig. 2h1-h2
9		LTK/2101-14 (BSIP 42259)	87.77	57.78	1.52			-
10	M3 (Elliptical)	LTK/2101-88 (BSIP 42262)	31.68	23.14	1.37	29.71	22.58	Fig. 3a1-a2
11		LTK/2101-21 (BSIP 42263)	27.74	22.01	1.26			Fig. 3b1-b3
12	M4 (Cylindrical)	LTK/2101-15 (BSIP 42265)	59.78	42.39	1.41	40.42	30.93	Fig. 3c1-c2
13		VVK/BNP/GEO9 (BSIP 42264)	21.05	19.47	1.08			Fig. 3d
14	M5 (Irregular)	VVK/BNP/GEO10 (BSIP 42266)	36.66	13.33	2.75	-	-	Fig. 3e1-e2

781

782

783 **Table 1.** Measurements (length, width, length/width) data for the late Cretaceous
 784 (Maastrichtian) coprolites recovered from the intertrappean deposit at Lotkheri, central India.